IOP Publishing | Royal Swedish Academy of Sciences Physica Scripta

Phys. Scr. **91** (2016) 064002 (10pp) doi:10.1088/0031-8949/91/6/064002

Discrete filters for large-eddy simulation of forced compressible magnetohydrodynamic turbulence

A A Chernyshov and A S Petrosyan[1]

Space Research Institute of the Russian Academy of Sciences, Profsoyuznaya 84/32, 117997, Moscow, Russia

E-mail: achernyshov@iki.rssi.ru and apetrosy@iki.rssi.ru

Received 12 January 2016, revised 11 March 2016
Accepted for publication 5 April 2016
Published 3 May 2016

Abstract

We discuss results of the applicability of discrete filters for the large-eddy simulation (LES) method of forced compressible magnetohydrodynamic (MHD) turbulent flows with the scale-similarity model. New results are obtained for cross-helicity and residual energy. Cross-helicity and residual energy are important quantities in magnetohydrodynamic turbulence and have no hydrodynamic counterpart. The influences and effects of discrete filter shapes on the scale-similarity model are examined in physical space using finite-difference numerical schemes. We restrict ourselves to the Gaussian filter and the top-hat filter. Representations of this subgrid-scale model, which correspond to various 3- and 5-point approximations of both Gaussian and top-hat filters for different values of parameter ϵ (the ratio of the cut-off length-scale of the filter to the mesh size), are investigated. Discrete filters produce more discrepancies for the magnetic field. It is shown that the Gaussian filter is more sensitive to the parameter ϵ than the top-hat filter in compressible forced MHD turbulence. The 3-point filters at $\epsilon = 2$ and $\epsilon = 3$ give the least accurate results whereas the 5-point Gaussian filter shows the best results at $\epsilon = 2$ and $\epsilon = 3$. There are only very small differences deep into the dissipation region in favor of $\epsilon = 2$. For cross-helicity, the 5-point discrete filters are in good agreement with the results of direct numerical simulation (DNS), while the 3-point filter produces the largest discrepancies with DNS results. There is no strong dependence on the choice of the parameter ϵ and order approximation is a much more important factor for the cross-helicity. The difference between the filters is less for the residual energy compared with total energy. Thus, the total energy is more sensitive to the choice of discrete filter in the modeling of compressible MHD turbulence using the LES method.

Keywords: compressible mixing, subgrid-scale modeling, magnetohydrodynamic turbulence

1. Introduction

Compressible turbulent plasma flows in a magnetic fields are common both in engineering and applied areas, and in the physics of geophysical, space and astrophysical processes. Turbulent phenomena are observed in near-Earth plasma, both in solar wind and in different regions of the Earth's magnetosphere (for instance, geomagnetic tail, auroral zone, interplanetary medium, dynamo process and space magnetic field generation). Among the engineering applications, the possibility of boundary layer control and drug reduction, magnetohydrodynamic (MHD) flows in pipes for the cooling of nuclear fusion reactors and in channels for steel-casting processes can be mentioned. Most of the applications require an understanding of turbulent flow at high Reynolds numbers with density fluctuations due to compressibility (such as in aerospace engineering design). The presence of velocity and magnetic field fluctuations in a wide range of space and time scales have been directly detected in the various turbulent flows in space processes. For example, there are strong

[1] Author to whom any correspondence should be addressed.

indications of their presence in the solar corona, interplanetary medium, solar wind and others. Note that MHD problems differ from those of neutral fluid hydrodynamics. MHD equations contain two fields that introduce considerably more freedom into the dynamics. Fundamental limitations of the direct numerical simulation (DNS) method for turbulence modeling and difficulties owing to the presence of magnetic fields and compressibility require development of new computational and theoretical methods and make important the advancement of the large eddy simulation (LES) method for such complex MHD flows. According to LES theory, the large-scale part of the flow is immediately computed and only small-scale turbulent structures are modeled. This scale separation is achieved by applying a filter. The small-scale motion is eliminated from the initial equations of motion by filtering operations and its influence is taken into account by special closures usually referred to as the subgrid-scale (SGS) models [1–8].

Currently, much attention is being paid to the important basic component of the LES method, namely, the development of SGS models and verification of their applicability [21]. At the same time, a significantly lower number of efforts are being made in the direction of other important fundamental problem of the LES approach: filtering procedures and the methods of their computational implementation. This work is devoted to an in-depth study of the influence of filter shapes on the modeling results of compressible MHD turbulence.

A special challenge is the study of turbulent MHD flows in the presence of turbulent mixing. It may be difficult to choose the shape of the filter in the LES; universal scales of mixing in turbulent flows may differ from those of ambient turbulent flow. Thus, applying the LES method for such plasma flows requires a careful choice of filtering operations together with the development of SGS models. The properties of these discrete filters differ noticeably from those of the continuous filters that are the basis of analytical analysis [23]. Consequently, it is necessary to analyze discrete filters and to define the discrete filters with the required properties to guarantee a better consistency between continuous SGS parameterization and its discretized version, which will be utilized for the calculation.

Analytical investigations on SGS modeling are performed by executing filtering procedures that are determined as convolution products between the velocity field and the filter kernel. Such a determination is appropriate when dealing with numerical approaches such as spectral or pseudospectral, and is expensive when handled with local methods (finite elements, finite differences, finite volumes). Normally discrete test filters with compact stencils based on weighted averages are applied for local methods. The characteristics of the discrete filters differ substantially from those of the continuous filters as mentioned above. Therefore, the choice of discrete filters with the necessary properties is an actual problem. Results concerning discrete filters evaluation for time evolution of velocity and magnetic field are obtained in [9]. Indeed, subsequent studies are needed to understand the influence of discrete filters on the dynamics of cross-helicity and residual energy [10] since these physical characteristics are important for understanding compressible turbulent mixing. These key questions are first addressed in the present work. For completeness, we provide a brief description of the LES approach of compressible MHD turbulence based on [9].

We deal with the question of the effects and influences of different filter shapes on the scale-similarity model in the LES method for compressible forced MHD turbulent flows using finite-difference schemes. Recently, we have shown that the scale-similarity model for forced MHD turbulence can be used as a stand alone SGS closure as opposed to the decaying case [9]. Scale-similarity parametrization has obvious advantages, the main one being to the ability to accurately reproduce the correlation between the actual and model turbulent stress tensor for isotropic flow as well as for anisotropic fluid flow, and the absence of special model constants, in contrast to other SGS models. However, the scale-similarity model does not sufficiently dissipate energy and usually leads to inaccurate results in decaying turbulence, or blows up the simulation. However, the situation changes significantly when a forced turbulence is considered. In this case, subgrid modeling in the LES approach provides the correct stationary regime of the turbulence rather than guaranteeing proper energy dissipation. It has been shown that the scale-similarity model provides good accuracy, and the results of this SGS model agree well with the DNS results. If differences between the results obtained by the scale-similarity model and the Smagorinsky closure for velocity field are insignificant, then the differences are considerable for magnetic fields. For the magnetic field, discrepancies with the DNS results are substantially lower for scale-similarity model, while the Smagorinsky parametrization for the MHD case is more dissipative and the results of the Smagorinsky model are worse, in agreement with DNS [9]. The scale-similarity model is generally found to reproduce DNS results better.

The structure of the paper is the following. Section 2 describes the general features of the LES technique in physical space. The influence and sensitivity of discrete filter shapes on the scale-similarity model, test configurations and numerical analysis of the obtained results are specified in section 3. Finally, concluding remarks are given in section 4.

2. Large-eddy simulation of compressible forced MHD turbulence

In this section, we formulate the general features of the theory of the LES method for modeling of compressible forced MHD turbulent flows [9, 11].

In order to obtain the MHD equation system governing the motion of the filtered (or resolved) eddies, the large scales from the small ones are expanded. The LES technique relies on the definition of a filtering procedure, that is, a resolved (or large-scale) characteristic, denoted by an overbar in this work, and is determined as

$$\bar{\zeta}(x) = \int_{\Theta} \zeta(x')\xi(x, x'; \bar{\Delta})\mathrm{d}x', \tag{1}$$

where ξ is the filter function satisfying the normalization property, ζ is a flow parameter, Θ is the domain, $\bar{\Delta}$ is the filter width associated with the wavelength of the smallest scale retained by the filtering procedure and $x_j = (x, y, z)$ are axes of the Cartesian coordinate system.

It is reasonable to apply the so-called Favre filtration (it is often called mass-weighted filtration) to avoid extra SGS terms due to compressibility effects. Thus, mass-weighted filtering will be used. Favre filtering is applied for all parameters of charged fluid flow in addition to the pressure and magnetic fields and is defined as follows:

$$\tilde{\zeta} = \frac{\overline{\rho\zeta}}{\bar{\rho}} \tag{2}$$

where the tilde denotes the mass-weighted filtration.

Hence, using the Favre-filtering operation, the MHD equations for compressible fluid flow can be rewritten as [9, 11]:

$$\frac{\partial\bar{\rho}}{\partial t} + \frac{\partial\bar{\rho}\tilde{u}_j}{\partial x_j} = 0; \tag{3}$$

$$\frac{\partial\bar{\rho}\tilde{u}_i}{\partial t} + \frac{\partial}{\partial x_j}\left(\bar{\rho}\tilde{u}_i\tilde{u}_j + \frac{\bar{\rho}^\gamma}{\gamma M_s^2}\delta_{ij} - \frac{1}{Re}\,\tilde{\sigma}_{ij} + \frac{\bar{B}^2}{2M_a^2}\delta_{ij} - \frac{1}{M_a^2}\,\bar{B}_j\bar{B}_i\right) = -\frac{\partial\tau^u_{ji}}{\partial x_j} + \tilde{F}_i^u; \tag{4}$$

$$\frac{\partial\bar{B}_i}{\partial t} + \frac{\partial}{\partial x_j}(\tilde{u}_j\bar{B}_i - \tilde{u}_i\bar{B}_j) - \frac{1}{Re_m}\frac{\partial^2\bar{B}_i}{\partial x_j^2} = -\frac{\partial\tau^b_{ji}}{\partial x_j} + \tilde{F}_i^b; \tag{5}$$

$$\frac{\partial\bar{B}_j}{\partial x_j} = 0, \tag{6}$$

since $\overline{\eta B_j} - \bar{\eta}\bar{B}_j = 0$ and $\bar{\sigma}_{ij} - \tilde{\sigma}_{ij} = 0$ [12], where $\tilde{\sigma}_{ij} = 2\tilde{\mu}\tilde{S}_{ij} - \frac{2}{3}\tilde{\mu}\tilde{S}_{kk}\delta_{ij} + \tilde{\zeta}\tilde{S}_{kk}\delta_{ij}$, and $\bar{\sigma}_{ij} = 2\overline{\mu S_{ij}} - \frac{2}{3}\overline{\mu S_{kk}\delta_{ij}} + \overline{\zeta S_{kk}\delta_{ij}}$. In numerical simulations, one usually neglects the last term by assuming the volume viscosity coefficient ζ to be equal to zero.

In relations (3)–(6), ρ is the density, u_j is the velocity in the direction x_j, B_j is the magnetic field in the direction x_j, $\sigma_{ij} = 2\mu S_{ij} - \frac{2}{3}\mu S_{kk}\delta_{ij}$ is the viscous stress tensor, $S_{ij} = 1/2(\partial u_i/\partial x_j + \partial u_j/\partial x_i)$ is the strain rate tensor, μ is the coefficient of molecular viscosity, η is the coefficient of magnetic diffusivity, and δ_{ij} is the Kronecker delta.

The filtered magnetohydrodynamic equations (3)–(6) are written in the dimensionless form using the standard procedure [2] where $Re = \rho_0 u_0 L_0/\mu_0$ is the Reynolds number, and $Re_m = u_0 L_0/\eta_0$ is the magnetic Reynolds number. $M_s = u_0/c_s$ is the Mach number, where c_s is the velocity of sound defined by the relation $c_s = \sqrt{\gamma p_0/\rho_0}$, and $M_a = u_0/u_a$ is the magnetic Mach number, where $u_a = B_0/(\sqrt{4\pi\rho_0})$ is the Alfvén velocity. To close the MHD equations (3)–(5) it is assumed that the relationship between density and pressure is polytropic and has the following form: $p = \rho^\gamma$, where γ is a polytropic index.

Note that mass-weighted filtration is used for all parameters of charged fluid motion except for the pressure and magnetic field. The magnetic field, as well as density and pressure, is filtered in the traditional way to avoid the complication of calculations because the MHD equations (3)–(6) do not contain products of the density and the magnetic field.

The effect of the SGSs appears on the right-hand side of the governing MHD equations (4)-(5) through the SGS stresses:

$$\tau^u_{ij} = \bar{\rho}(\widetilde{u_i u_j} - \tilde{u}_i\tilde{u}_j) - \frac{1}{M_a^2}(\overline{B_i B_j} - \bar{B}_i\bar{B}_j); \tag{7}$$

$$\tau^b_{ij} = (\overline{u_i B_j} - \tilde{u}_i\bar{B}_j) - (\overline{B_i u_j} - \bar{B}_i\tilde{u}_j). \tag{8}$$

Thus, the filtered system of MHD equations includes the unknown turbulent tensors τ^u_{ij} and τ^b_{ij}. To define their components, special turbulent models (or closures, or parameterizations) based on large-scale values describing turbulent MHD flow should be utilized. The central concept of any SGS models used in the LES technique is to reproduce the effects of the SGS dynamics on large-scale energy distribution, as does the Richardson turbulent cascade simulation. One ought to find closures for the terms τ^u_{ij} and τ^b_{ij} that would relate these tensors to the known large-scale values of the flow parameters in order to close the MHD equation system. Note that the trace of SGS stresses in compressible fluid flows cannot be contained in the modified pressure, and demands separate modeling, but it is very frequently neglected [12, 13]. Therefore, there is no additional need to close the often neglected turbulent magnetic pressure [5].

Any turbulent SGS tensor can be decomposed into three parts [14], for instance, for τ^u_{ij}:

$$\begin{aligned}\tau^u_{ij} &= \bar{\rho}(\widetilde{u_i u_j} - \tilde{u}_i\tilde{u}_j) - \frac{1}{M_a^2}(\overline{B_i B_j} - \bar{B}_i\bar{B}_j)\\ &= \underbrace{\bar{\rho}(\widetilde{\tilde{u}_i\tilde{u}_j} - \tilde{u}_i\tilde{u}_j) - \frac{1}{M_a^2}(\overline{\bar{B}_i\bar{B}_j} - \bar{B}_i\bar{B}_j)}_{\text{Leonard term}}\\ &\quad + \underbrace{\bar{\rho}(\widetilde{\tilde{u}_i u_j''} + \widetilde{\tilde{u}_j u_i''}) - \frac{1}{M_a^2}(\overline{\bar{B}_i B_j'} + \overline{\bar{B}_j B_i'})}_{\text{Cross term}}\\ &\quad + \underbrace{\bar{\rho}(\widetilde{u_i'' u_j''}) - \frac{1}{M_a^2}(\overline{B_i' B_j'})}_{\text{Reynolds-Maxwell term}}\\ &= L_{ij} + C_{ij} + R_{ij}.\end{aligned} \tag{9}$$

In expression (9), the Leonard stress L_{ij} describes the interaction between the resolved scales [14]. The cross term C_{ij} represents the interaction between the resolved and SGS motion. Finally, the third term, R_{ij}, the Reynolds–Maxwell stress tensor, describes the interaction between the SGSs and is responsible for energy dissipation. In general, there are two main approaches to turbulent stress modeling in LES. The first one is called scale similarity. It concentrates the attention at the Leonard term L_{ij}, that is, SGS tensors are proportion the Leonard stress tensor $\tau_{ij} \propto L_{ij} \propto L_{ij} + C_{ij} + R_{ij}$. The second approach is called eddy viscosity. It focuses on the Reynolds (or Reynolds–Maxwell) term R_{ij} and assumes that $\tau_{ij} \propto R_{ij}$.

The SGS Reynolds stress tensor is separated into deviatoric and isotropic parts. In this case, an eddy-viscosity assumption is used. The eddy-viscosity model is defined in general view as:

$$\tau_{ij}^{u} - \frac{1}{3}\tau_{kk}^{u}\delta_{ij} = -2\nu_t\left(\tilde{S}_{ij} - \frac{1}{3}\tilde{S}_{kk}\delta_{ij}\right), \quad (10)$$

$$\tau_{ij}^{b} - \frac{1}{3}\tau_{kk}^{b}\delta_{ij} = -2\eta_t\bar{J}_{ij}. \quad (11)$$

Here ν_t and η_t are scalar turbulent functions depending on spatial coordinates and time, $\tilde{S}_{ij} = \frac{1}{2}(\partial\tilde{u}_i\partial x_j + \partial\tilde{u}_j\partial x_i)$ is a large-scale strain rate tensor, and $\bar{J}_{ij} = \frac{1}{2}(\partial\bar{B}_i\partial x_j - \partial\bar{B}_j\partial x_i)$ is a large-scale magnetic rotation tensor.

The symmetric terms comprising the magnetic rate-of-strain tensor $\bar{S}_{ij}^{b} = (\partial\bar{B}_i/\partial x_j + \partial\bar{B}_j/\partial x_i)/2$ and the vorticity tensor $\tilde{J}_{ij}^{u} = (\partial\tilde{u}_i/\partial x_j - \partial\tilde{u}_j/\partial x_i)/2$ are omitted on the right-hand sides of the equations (10) and (11), respectively, since their influence is negligible, as shown in [5].

The term $\frac{1}{3}\tau_{kk}^{u}\delta_{ij}$ is often neglected and is related to the thermodynamic pressure $\nabla\left(p + \frac{2}{3}k\delta_{ij}\right)$ (see [15]), where $k = (\tau_{11} + \tau_{22} + \tau_{33})/2$ is the SGS turbulent kinetic energy. However, as indicated in papers [3, 4, 9, 11, 16], the general case when the SGS isotropic term is taken into account using realizability conditions is considered.

In the present work, the scale-similarity model is applied. The scale-similarity model is not of the eddy-viscosity type. It is based on the assumption that the largest unresolved scales are similar to the smallest resolved scales of turbulent flow and uses the filter twice to separate the smallest and largest resolved scales. The largest unresolved scales are approximated by the smallest resolved scales, for example, for the velocity: $u_i'' \approx \tilde{u}_i'' \approx \tilde{\tilde{u}}_i - \tilde{u}_i$. The scale-similarity model as a SGS closure for the compressible MHD case is of the form [16]:

$$\tau_{ij}^{u} = \bar{\rho}(\widetilde{\tilde{u}_i\tilde{u}_j} - \tilde{\tilde{u}}_i\tilde{\tilde{u}}_j) - \frac{1}{M_a^2}(\overline{\bar{B}_i\bar{B}_j} - \bar{\bar{B}}_i\bar{\bar{B}}_j) \quad (12)$$

$$\tau_{ij}^{b} = (\overline{\tilde{u}_i\bar{B}_j} - \tilde{\tilde{u}}_i\bar{\bar{B}}_j) - (\overline{\bar{B}_i\tilde{u}_j} - \bar{\bar{B}}_i\tilde{\tilde{u}}_j). \quad (13)$$

The scale-similarity model for MHD turbulence (12) and (13) may be computed with the help of the filtered variables in contrast to eddy-viscosity parameterizations. Model constants in (12) and (13) are not introduced as this would destroy the Galilean invariance of the expression [17]. This is the main advantage of scale-similarity closure. It has been shown that the scale-similarity model provides good accuracy and the results of this SGS model agree well with the DNS results for forced compressible MHD turbulence [9].

There are external driving forces F_i^u and F_i^b on the right-hand sides of expressions (4) and (5), respectively. Driving forces F_i^u and F_i^b, which sustain turbulence, are necessary to study statistically stationary flow and ensure a stationary picture of the energy cascade and more statistical sampling. If energy is not injected into a turbulent flow, after some time this turbulent flow becomes laminar due to viscosity and diffusion. In order to sustain three-dimensional turbulence, a driving force is employed to inject energy in the turbulent system to replace the energy that is dissipated on small spatial scales.

Recently, 'linear forcing' was suggested and used for modeling compressible MHD turbulence [11], with a driving force in physical space. The idea essentially consists of adding a force proportional to the fluctuating velocity [11, 18–21]. Linear forcing resembles a turbulence when forced with a mean velocity gradient, i.e. a shear. This driving force appears as a term in the expression for fluctuating velocity that conforms to a production term in the equation of turbulent kinetic energy. In compressible MHD turbulence, an MHD equation system also includes a magnetic induction expression, and in this case the external force is proportional to the magnetic field in the magnetic induction equation [11]. Thus, this driving force may be explained as the production of magnetic energy owing to the interaction between the magnetic field and the mean fluid shear.

The determination of the driving forces F_i^u and F_i^b in the momentum conservation equation and in the magnetic induction equation, respectively, is given by:

$$F_i^u = \Theta\rho u_i \quad (14)$$

$$F_i^b = \Psi B_i \quad (15)$$

where Θ in (14) is the coefficient that is defined from a balance of kinetic energy for a statistically stationary state. The forcing function $F_i^u = \Theta\rho u_i$ in physical space is equivalent to the force of all the Fourier modes in spectral space. This is in fact the only difference from standard spectral forcing when energy is added into the system only in the range of small wave numbers (wave number shell), that is, in integrated (large) scale of turbulence. The coefficient Ψ in expression (15) is also determined from the balance of magnetic energy for the statistically stationary state. The parameter Ψ is specified as $\Psi = \chi/3B_{rms}^2$, where $\chi = \langle\eta B_i(\partial^2 B_i/\partial x_j^2)\rangle$ is resistive dissipation of the turbulent magnetic energy in MHD turbulence and $B_{rms}^2 = \langle B^2\rangle/3$ is the root-mean-square magnetic field. Just like the parameter Θ in expression (14), the coefficient Ψ in relation (15) can be constant as well as recalculated on each time step during modeling of MHD turbulence with driving force. More detailed derivation and information about the linear forcing method in physical space for compressible MHD turbulent flows can be found in our article [11].

3. Sensitivity of cross-helicity and residual energy on the filter shape and comparisons with that for turbulent spectra

In this section, the influences and sensitivity of discrete filter shapes on the scale-similarity model for MHD turbulence for cross-helicity and residual energy are studied. Test configurations and numerical analysis of obtained results are present. The results obtained for the LES technique are compared with the DNS results for three-dimensional forced compressible MHD turbulent flows. Comparisons are made with results for turbulent spectra obtained in [9].

We begin with a brief description of derivations of various discrete filters in the LES approach for the sake of clarity.

There is an evident effect of the properties of the LES filter on the interactions between resolved and subgrid scales. We examine the question of the effect of different filter shapes on the scale-similarity model for forced compressible MHD turbulent flow using finite-difference schemes. Several papers have been devoted to this problem for neutral fluids dynamics. Both theoretical and numerical studies have been carried out [22–24].

It should be remarked that the definition of the filtering procedure (1) is too general. The real flows in nature and in experiments can be investigated with the help of some simpler appropriate filter. Note that the operator specified by (1) is *a priori* non-local in physical space, and then is not appropriate for calculations performed with local numerical methods (e.g. finite elements, finite volumes and finite differences). Therefore, there is a need to determine some local discrete approximations for this operator. Since the finite-difference schemes for the simulation of MHD turbulent flows are used in this paper, we consider the Gaussian filter and the top-hat (or box) filter. They are commonly applied when using non-spectral modeling techniques in physical space. The filters can be expressed in discrete form for practical consideration. To do that, it is necessary to define the differential operator associated with the filter in (1). Using the Taylor expansion, we have the following:

$$\zeta(\acute{x}) = \zeta(x) + \sum_{l=1}^{\infty}\frac{(\acute{x}-x)^l}{l!}\frac{\partial^l\zeta(x)}{\partial x^l}. \qquad (16)$$

Introducing this expansion into (1), we obtain for the filtered variable:

$$\bar{\zeta}(x) = \zeta(x) + \sum_{l=1}^{\infty}\frac{(-1)^l K_l\bar{\Delta}^l}{l!}\frac{\partial^l\zeta(x)}{\partial x^l} \qquad (17)$$

where K_l is the moment of order l of the kernel ξ, that is, $K_l = \int_\Theta \xi(\acute{x})\acute{x}^l \mathrm{d}\acute{x}$.

The differential form (17) is well posed if and only if $|K_l| < \infty$ for $\forall\, l$, implying that the kernel ξ quickly diminishes in space and $\bar{\Delta}$ is the characteristic cut-off length-scale connected with the LES filter [1]. Two filters are classically applied for analytical studies in the LES method in physical space, which satisfy that the criteria are the top-hat filter and the Gaussian filter.

The top-hat filter is defined as:

$$\xi(x, \acute{x}) = \begin{cases} \frac{1}{\bar{\Delta}}, & \text{if} |x-\acute{x}| \leqslant \frac{\bar{\Delta}}{2}. \\ 0, & \text{otherwise} \end{cases} \qquad (18)$$

The corresponding differential operator is

$$\tilde{\zeta}(x) = \zeta(x) + \frac{\bar{\Delta}^2}{24}\Lambda(\zeta) + \frac{\bar{\Delta}^4}{1920}\Lambda^2(\zeta) + \frac{\bar{\Delta}^6}{322560}\Lambda^4(\zeta) + O(\bar{\Delta}^8) \qquad (19)$$

where $\Lambda(\zeta) = \partial^2\zeta/\partial(x)^2$ is a Laplacian operator.

The Gaussian filter is:

$$\xi(x, \acute{x}) = \left(\frac{6}{\pi\bar{\Delta}^2}\right)^{1/2}\exp\left(-\frac{6|x-\acute{x}|^2}{\bar{\Delta}^2}\right)^{1/2}\Bigg). \qquad (20)$$

For the Gaussian filter, the corresponding differential approximation takes the form:

$$\begin{aligned}\tilde{\zeta}(x) &= \zeta(x) + \frac{\bar{\Delta}^2}{24}\Lambda(\zeta) + \frac{\bar{\Delta}^4}{1152}\Lambda^2(\zeta) \\ &\quad + \frac{\bar{\Delta}^6}{82944}\Lambda^4(\zeta) + O(\bar{\Delta}^8).\end{aligned} \qquad (21)$$

The associated discrete operator equivalent to the nth order of the filter is derived by discretizing the aforementioned differential operators.

The filter approach for the hydrodynamics of neutral gas was analyzed by Sagaut and Grohens [23]. They were looking for an optimal shape of the filters that is consistent with the numerical scheme in use. They found, by means of the Taylor series decomposition, that the top-hat and Gaussian filters coincide exactly for second-order accuracy numerical schemes (using 3-points):

$$\bar{\zeta}_i = \frac{1}{24} * \epsilon^2 * \zeta_{i-1} + \frac{1}{12} * (12-\epsilon^2) * \zeta_i + \frac{1}{24} * \epsilon^2 * \zeta_{i+1} \qquad (22)$$

Fourth-order accuracy numerical schemes (using 5-points) are consistent with different forms of these filters. Operators equivalent to the fourth-order Gaussian filter and top-hat filter respectively are:

$$\begin{aligned}\bar{\zeta}_i = &\frac{\epsilon^4 - 4\epsilon^2}{1152}(\zeta_{i-2} + \zeta_{i+2}) \\ &+ \frac{16\epsilon^2 - \epsilon^4}{288}(\zeta_{i-1} + \zeta_{i+1}) + \frac{\epsilon^4 - 20\epsilon^2 + 192}{192}\zeta_i,\end{aligned} \qquad (23)$$

$$\begin{aligned}\bar{\zeta}_i &= \frac{3\epsilon^4 - 20\epsilon^2}{5760}(\zeta_{i-2} + \zeta_{i+2}) \\ &\quad + \frac{80\epsilon^2 - 3\epsilon^4}{1440}(\zeta_{i-1} + \zeta_{i+1}) \\ &\quad + \frac{3\epsilon^4 - 100\epsilon^2 + 960}{960}\zeta_i.\end{aligned} \qquad (24)$$

Here, ζ_i is the flow parameter in the point i and the parameter ϵ represents the the ratio of cut-off length-scale of

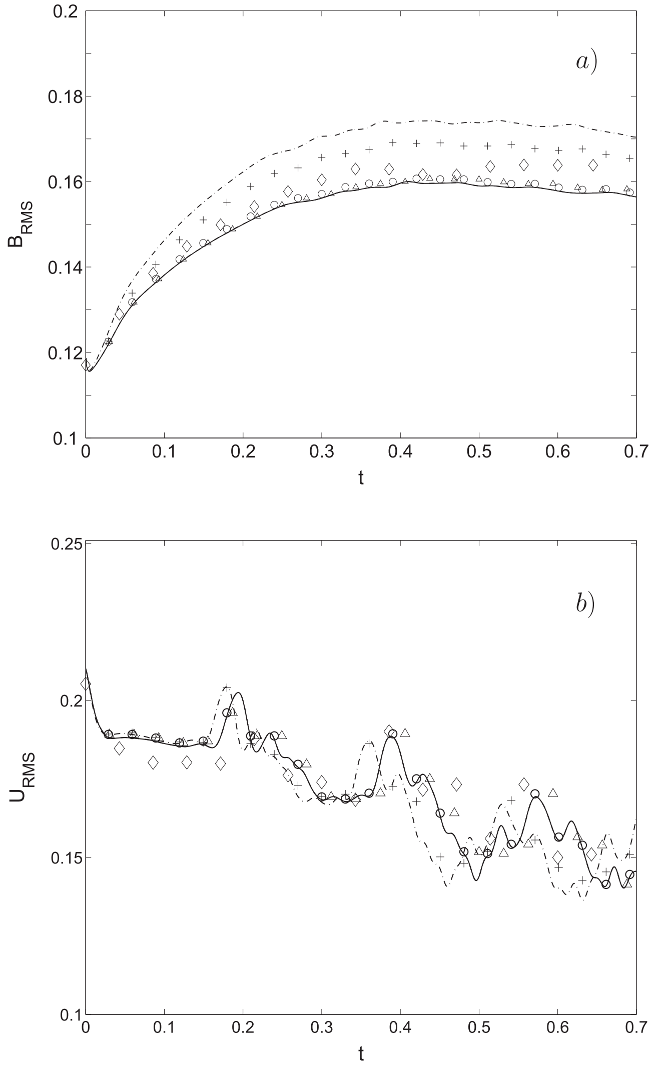

Figure 1. Time dynamics of b_{rms} (a) and u_{rms} (b) for various filter shapes. The diamond symbol denotes the DNS results, the solid line is the 5-point approximation of the Gaussian filter ($\epsilon = 2$), the dashed line is the 5-point approximation of the top-hat filter ($\epsilon = 2$), the dash-dot line is the 3-point approximation of the Gaussian (or top-hat) filter ($\epsilon = 2$), the circle symbol is the 5-point approximation of the Gaussian filter ($\epsilon = 3$), the triangle symbol is the 5-point approximation of the top-hat filter ($\epsilon = 3$), and the plus symbol is the 3-point approximation of the Gaussian (or top-hat) filter ($\epsilon = 3$).

the filter to the mesh size. It is usually assumed that the parameter ϵ is equal to 2 in the works where the fluid flows are modeled by means of the LES approach. However, in order to study how this parameter affects the results of the calculations, we consider the cases when the parameter ϵ takes a different value, namely, $\epsilon = 3$.

Initially it should be noted that since the problem considered in this paper is three-dimensional, a three-dimensional filter (a multidimensional one in the general case) should be designed. A multidimensional filter may be designed in two different modes [23]. The first one is a linear combination of one-dimensional filters. For every direction the flow parameter is filtered independently from the others:

$$\xi^n = \frac{1}{n}\sum_{i=1}^{n}\xi^i, \tag{25}$$

where ξ^i is a one-dimensional filter in direction i, and n is the number of space dimensions. Linear combination corresponds to simultaneous application of all one-dimensional filters in every spatial direction. The second approach represents a product of one-dimensional filters:

$$\xi^n = \prod_{i=1}^{n} \xi^i. \tag{26}$$

Such method of definition of multidimensional filter ξ^n corresponds to non-simultaneous application of one-dimensional filters such as in the first case but a sequential one. The precision of designed multidimensional filters was explored by Sagaut and Grohens [23]. It was demonstrated that sequential product of filters provides more accurate results in comparison with the linear combination of one-dimensional filters. Consequently, the sequential product of filters (26) is applied for three-dimensional filtration in this study.

Three-dimensional numerical simulations of forced compressible MHD turbulence in physical space were performed and the numerical code of the fourth-order accuracy for MHD equations in the conservative form based on non-spectral finite-difference schemes is used in our work. The third-order low-storage Runge–Kutta method is applied for time integration. The skew-symmetric form of nonlinear terms for modeling of turbulent flow is applied to reduce discretization errors. The skew-symmetric form is a form obtained by averaging divergent and convective forms of the nonlinear terms:

$$\Psi_i^s = \frac{1}{2}\left(\frac{(\partial\rho u_i u_j)}{\partial x_j} + \rho u_j\frac{\partial u_i}{\partial x_j} + u_i\frac{(\partial\rho u_j)}{\partial x_j}\right). \tag{27}$$

Despite the analytical equivalence of all three forms, their numerical realizations ensure different results. In [25], the authors asserted that the skew-symmetric form improves computational accuracy for turbulent modeling. Periodic boundary conditions for all three dimensions are used. The similarity numbers in all simulations are: $Re \approx 300$, $Re_M \approx 50$, $M_s \approx 0.35$, $M_a \approx 1.4$, $\gamma = 1.5$. The modeling domain is a cube $\pi \times \pi \times \pi$. A mesh with 64^3 grid cells is used for LES and 256^3 for DNS. The explicit LES method is used in the present study. The initial isotropic turbulent spectrum close to k^{-2} with random phases and amplitudes in all three directions was selected for magnetic and kinetic energy in Fourier space. The choice of such a spectrum for the initial conditions is the result of velocity perturbations with an initial power spectrum in Fourier space similar to that of developed turbulence [26]. It should be noted that the k^{-2} spectrum corresponds to the spectrum of Burgers turbulence. Initial conditions for the magnetic field and the velocity were derived in physical space by inverse Fourier transform. The results obtained with the LES technique are compared with DNS calculations and the LES performance is studied using the difference between LES and filtered DNS results. The initial conditions for LES are obtained by filtering the initial conditions of DNS.

Since our interest is in study scale-similarity SGS parameterizations that depend on the application of a filter to its discrete statement, we consider various versions of scale-similarity closure that correspond to various 3- and 5-point approximations of both Gaussian and top-hat filters for $\epsilon = 2$ and $\epsilon = 3$.

The time dynamics of root-mean-square magnetic field b_{rms} and root-mean-square velocity u_{rms} are shown in figures 1(a) and (b), respectively. Here and below, in figure 1, the diamond symbol denotes the DNS results, the solid line is the 5-point approximation of the Gaussian filter ($\epsilon = 2$), the dashed line is the 5-point approximation of the top-hat filter ($\epsilon = 2$), the dash-dot line is the 3-point approximation of the Gaussian (or top-hat) filter ($\epsilon = 2$), the circle symbol is the 5-point approximation of the Gaussian filter ($\epsilon = 3$), the triangle symbol is the 5-point approximation of the top-hat filter ($\epsilon = 3$), and the plus symbol is the 3-point approximation of the Gaussian (or top-hat) filter ($\epsilon = 3$). In these plots, we can see that the use of the 5-point filters leads to an increase in the accuracy. The largest discrepancy with the DNS results is observed for scale-similarity results with the 3-point Gaussian (or top-hat) filters at different values of ϵ. At the same time, the 5-point filters agree well with the 'exact' DNS results. Note that 5-point discrete filters lead to similar results for the two values of parameter ϵ, whereas a 3-point filter produces more discrepancies for magnetic fields. Note that the dash-dot line coincides with the dashed line in figure 1, that is, results for the 3-point approximation of the top-hat filter ($\epsilon = 2$) agree very closely with the results of the 5-point approximation of the top-hat filter ($\epsilon = 2$).

The spectral distribution of the magnetic and kinetic energies demonstrates redistribution of energy depending on wave number, in other words, at different scales. The investigation of inertial range properties is one of the principal problems in studies of scale-similarity spectra of MHD turbulence. Inertial range properties are determined as time averages over periods of stationary turbulence conditions. It is worth noting that the well-known spectra of Iroshnikov–Kraichnan and Kolmogorov–Obukhov for MHD turbulence in inertial range were derived precisely for the total energy. That is why the total energy is a key parameter for proper filter selection. The total energy is the sum of the magnetic and kinetic energies $E_T = E_M + E_K$. The spectra of total energy E_T^K conforming to these various cases are depicted in figure 2(a). As expected from the theory of the LES method, the main differences in the results are concentrated on the small (unresolved) scales. In order to observe these differences better, for the sake of clarity, figure 2(b) shows an enlarged zone for large values of wave number k. It should be noted that the Gaussian filter is more sensitive to the parameter ϵ than the top-hat one for the scale-similarity model in compressible MHD turbulence. From our calculations it can be seen that the 3-point filters give the worst results and the 5-point Gaussian filter demonstrates the best results (that is, the best approximation to DNS) at $\epsilon = 2$. However, the difference between these filters is still within 10%.

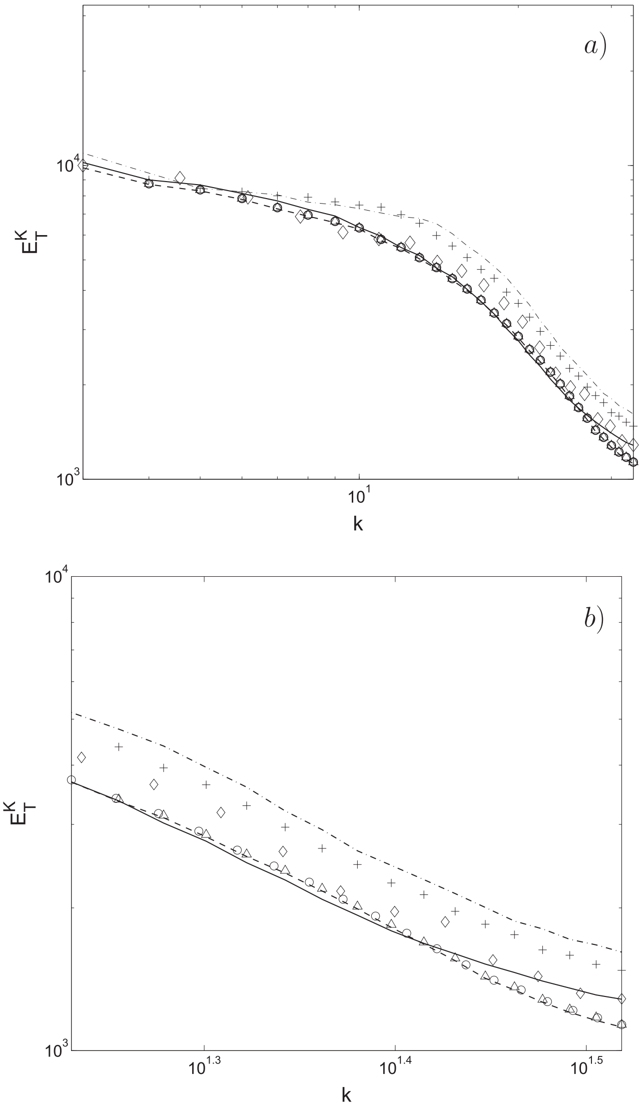

Figure 2. (a) Total energy spectrum E_T^K, (b) total energy spectrum E_T^K in an enlarged zone for large values of wave number k. Symbols are the same as in figure 1.

There is a quantity than plays an important role in MHD turbulence, namely the difference between the magnetic and the kinetic energies, called residual energy $E_R = |E_M - E_K|$. The residual energy establishes a direct link between the kinetic and magnetic energies in MHD turbulent flow [27]. The residual energy spectrum is a fundamental parameter that is expected to follow a power law together with the total energy spectrum. Figure 3(a) shows the residual energy spectrum $E_R^K = |E_M^K - E_K^K|$ for various filter shapes. To better see the differences at large wave numbers k in the spectral space, as well as for the total energy spectrum above, we present figure 3(b) with an enlarged zone for large values of wave number. Note that the 3-point top-hat and 3-point Gaussian filters produce the least accurate result, which is in

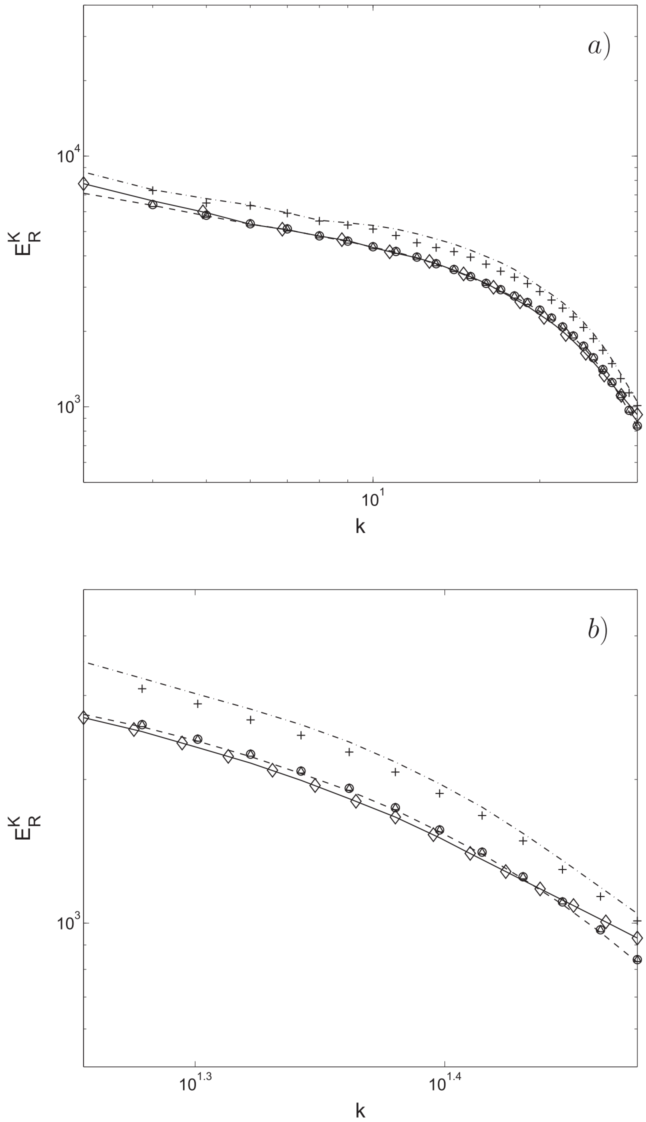

Figure 3. (a) Residual energy spectrum $E_R^K = |E_M^K - E_K^K|$, (b) residual energy spectrum E_R^K in an enlarged zone of large values of wave numbers k for various filter shapes. Symbols are the same as in figure 1.

good agreement with the results of the total energy spectrum. In addition, similar to the total energy spectrum, as indicated above, the 5-point Gaussian discrete filter at $\epsilon = 2$ shows very good results. It is necessary to notice that the difference between all considered filters is less for the residual energy compared with the total energy for large values of wave number k exactly for the scales that are important in LES. In other words, the residual energy is less sensitive to the choice of filter in the modeling of compressible MHD turbulence using the LES technique.

An important quantity in MHD of charged fluids is an evolution of cross-helicity $H^c = \int_V (uB)\mathrm{d}V$. There are self-organization processes in MHD turbulence that have no hydrodynamic counterpart and it is often necessary to consider the dynamics of cross-helicity for the study of such processes. In figure 4, the time evolution of the cross-helicity

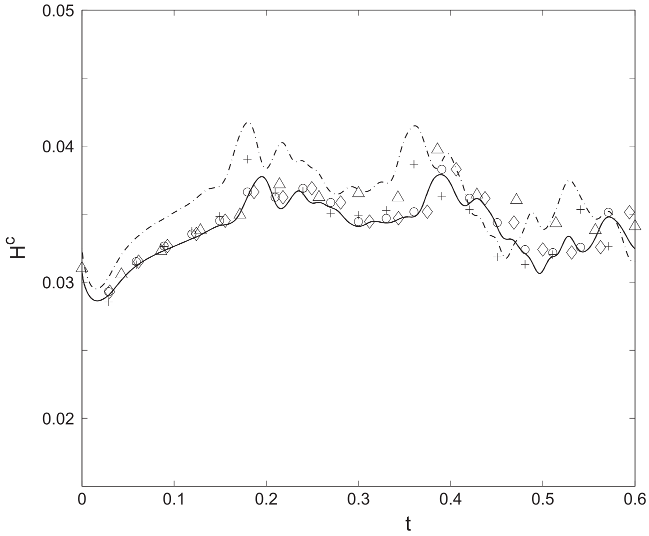

Figure 4. Time evolution of the cross-helicity H^c for various filter shapes. Symbols are the same as in figure 1.

H^c is plotted. Note that the 5-point discrete filters are in good agreement with the results of DNS while the 3-point filter produces the largest discrepancies with DNS results. In our runs, there is no strong dependence on the choice of the parameter ϵ and order approximation is much more important factor for cross-helicity.

4. Concluding remarks

This work concerns the study of the impact of discrete filter shapes on the results of numerical investigations of compressible MHD turbulence using the LES method. This issue is crucial in modeling a wide class of turbulent flows in hydrodynamics and plasma. This is especially true of turbulent flows in the presence of mixing. The conclusions can be used to understand the complex physics accompanied by such phenomena.

In the LES method, the filtering procedure is applied to the governing equation system. Each physical parameter is expanded into large- and small-scale components. The effects on large scales are computed directly and those on small scales are modeled. In other words, the information on turbulent structures with sizes smaller than the filter width is lost during the filtering procedure, therefore various SGS models are used to close the filtered system of equations. Filtering operators can be introduced in explicit and implicit forms. In the implicit approach, the filtering operator is represented by difference discretization and in this case the filtering scales are smaller than the grid step. Shortcomings of implicit filtering are related to difficulties in comparing the results obtained with direct numerical simulation and experimental data. Additionally, implicit filtering does not allow control over the high-frequency spectral range, which can lead to numerical errors. Thus, explicit filtering is preferable in the LES technique. Therefore it is important to understand how discrete filters affect the study of turbulence flows, especially in the presence of magnetic fields.

It appears that parameter ϵ, which represents the ratio of the cut-off length-scale of the filter to the mesh size, is an important parameter regarding the discrete filters of the LES approach as well as the order of the discrete filters. The present study summarizes results concerning discrete filters for the LES method of forced compressible MHD turbulent flows with the scale-similarity model. Scale-similarity parametrization has evident advantages in forcing compressible turbulence. The influences and effects of discrete filter shapes on the scale-similarity model were examined in physical space using a finite-difference numerical schemes. In this paper, the obtained results of modeling for LES were compared with the DNS results of three-dimensional compressible forced MHD turbulent flows. The comparison between LES and DNS results was carried out regarding the evolution of b_{rms}, u_{rms} and the cross-helicity, and the total energy spectra and residual energy spectrum of compressible MHD turbulence. It was shown that the Gaussian filter is more sensitive to the parameter ϵ than the top-hat filter for the scale-similarity model in compressible MHD turbulent fluid flow. A noteworthy result is that discrete filters produce more discrepancies for magnetic fields. Therefore, it is important to choose correctly a filter using the LES approach for modeling of forced compressible MHD turbulence. For cross-helicity, the 5-point discrete filters provide good agreement with the results of DNS, while the 3-point filter produces the largest discrepancies with DNS results. We conclude that there is no strong dependence on the choice of the parameter ϵ and order approximation is a much more important factor for cross-helicity. In general, the 3-point filters at $\epsilon = 2$ and $\epsilon = 3$ give the least accurate results and the 5-point Gaussian filter shows the best results at $\epsilon = 2$ and $\epsilon = 3$. There are only very small differences deep into the dissipation region in favor of $\epsilon = 2$. The difference between discrete filters is within 10%. As expected, the main differences in the results are concentrated on the small scales for the energy spectrum. The difference between filters is less for the residual energy compared with the total energy for large values of wave number k, that is, the total energy is more sensitive to the choice of a discrete filter for modeling of compressible MHD turbulence by means of the LES method.

The results obtained in this study have importance for the choice of discrete filters in large eddy simulations of turbulent mixing processes in MHD.

Acknowledgments

The work was partly supported by grants from the Russian Foundation for Basic Research (14-02-31848, 14-29-06065) and by Program #9 of the Russian Academy of Science Presidium 'Experimental and theoretical studies of solar system objects and stellar planetary systems'. ACh gratefully acknowledges support from the grant of President of Russian Federation (MK-267.2014.5).

References

[1] Garnier E, Adams N and Sagaut P 2009 *Large Eddy Simulation for Compressible Flows* (Dordrecht: Springer)
[2] Biskamp D 2003 *Magnetohydrodynamic turbulence* (United Kingdom: Cambridge University Press)
[3] Chernyshov A A, Karelsky K V and Petrosyan A S 2006 Large-eddy simulation of magnetohydrodynamic turbulence in compressible fluid *Phys. Plasmas* **13** 032304
[4] Chernyshov A A, Karelsky K V and Petrosyan A S 2008 Modeling of compressible magnetohydrodynamic turbulence in electrically and heat conducting fluid using large eddy simulation *Phys. Fluids* **20** 085106
[5] Müller W-C and Carati D 2002 Dynamic gradient-diffudion subgrid models for incompressible magnetohydrodynamics turbulence *Phys. Plasmas* **9** 824–34
[6] Chernyshov A A, Karelsky K V and Petrosyan A S 2009 Validation of large eddy simulation method for study of flatness and skewness of decaying compressible magnetohydrodynamic turbulence *Theor. Comput. Fluid Dyn.* **23** 451–70
[7] Chernyshov A A, Karelsky K V and Petrosyan A S 2006 Subgrid-scale modelling of compressible magnetohydrodynamic turbulence in heat-conducting plasma *Phys. Plasmas* **13** 104501
[8] Chernyshov A A, Karelsky K V and Petrosyan A S 2010 Novel developments in subgrid-scale modeling of space plasma: weakly compressible turbulence in the local interstellar medium *Phys. Scr.* **2010** 014029
[9] Chernyshov A A, Karelsky K V and Petrosyan A S 2012 Efficiency of scale-similarity model for study of forced compressible magnetohydrodynamic turbulence *Flow, Turbulence and Combustion* **89** 563–87
[10] Yokoi N 2006 Modeling of the turbulent magnetohydrodynamic residual-energy equation using a statistical theory *Phys. Plasmas* **13** 062306–062306-17
[11] Chernyshov A A, Karelsky K V and Petrosyan A S 2010 Forced turbulence in large eddy simulation of compressible magnetohydrodynamic turbulence *Phys. Plasmas* **17** 102307
[12] Piomelli U 1999 Large-eddy simulation: achievements and challenges *Prog. Aerosp. Sci.* **35** 335–62
[13] Zang T A, Dahlburg R B and Dahlburg J P 1992 Direct and large-eddy simulations of three-dimensional compressible navier-stokes turbulence *Phys. Fluids* A **4** 127–3140
[14] Leonard A 1974 Energy cascade in large eddy simulations of turbulent fluid flows *Adv. Geophys* **18** 237–48
[15] Erlebacher G, Hussaini M, Speziale C and Zang T 1992 Toward the large-eddy simulation of compressible turbulent flows *J. Fluid. Mech.* **238** 155–85
[16] Chernyshov A A, Karelsky K V and Petrosyan A S 2007 Development of large eddy simulation for modeling of decaying compressible mhd turbulence *Phys. Fluids* **19** 055106
[17] Speziale G 1985 Galilean invariance of subgrid-scale stress models in les of turbulence *J. Fluids Mech.* **156** 55–62
[18] Lundgren T S 2003 Linearly forced isotropic turbulence *Center for Turbulence Research Annual Research Briefs* 461–73 (https://ctr.stanford.edu/annual-research-briefs-2003)
[19] Rosales C and Meneveau C 2005 Linear forcing in numerical simulations of isotropic turbulence: physical space implementations and convergence properties *Phys. Fluids* **17** 095106

[20] De Stefano G and Vasilyev O V 2010 Stochastic coherent adaptive large eddy simulation of forced isotropic turbulence *J. Fluid Mechanics* **646** 453–70

[21] Chernyshov A A, Karelsky K V and Petrosyan A S 2014 Subgrid-scale modeling for the study of compressible magnetohydrodynamic turbulence in space plasmas *Phys.-Usp.* **57** 421

[22] Piomelli U, Ferziger J H and Moin P 1988 Model consistency in large eddy simulation of turbulent channel flows *Phys. Fluids* **31** 1884–91

[23] Sagaut P and Grohens R 1999 Discrete filters for large eddy simulation *Int. J. Numer. Mech. Fluids.* **31** 1195–220

[24] Leslie D C and Quarini G L 1979 The application of turbulence theory to the formulation of subgrid modelling procedures *J. Fluid Mech.* **91** 65–91

[25] Park N, Yoo J Y and Choi H 2004 Discretization errors in large eddy simulation: on the suitability of centered and upwind-biased compact difference schemes *J. of Comput. Phys.* **198** 580–616

[26] Mac Low M-M, Klessen R S, Burkert A and Smith M D 1998 Kinetic energy decay rates of supersonic and super-alfvenic turbulence in star-forming clouds *Phys. Rev. Lett.* **80** 2754–64

[27] Müller W-C and Grappin R 2004 The residual energy in freely decaying magnetohydrodynamic turbulence *Plasma Phys. Control. Fusion* **45** B91–6